Generalized seniority from random Hamiltonians

C. W. Johnson,[1] G. F. Bertsch,[2,3] D. J. Dean,[4] and I. Talmi[2,5]

[1]*Department of Physics and Astronomy, Louisiana State University, Baton Rouge, Louisiana 70803*
[2]*Institute for Nuclear Theory, University of Washington, Seattle, Washington 98195*
[3]*Department of Physics, University of Washington, Seattle, Washington 98195*
[4]*Physics Division, Oak Ridge National Laboratory, Oak Ridge, Tennessee 37831*
and Department of Physics and Astronomy, University of Tennessee, Knoxville, Tennessee 37996
[5]*Weizmann Institute of Science, Rehovot, Israel*

We investigate the generic pairing properties of shell-model many-body Hamiltonians drawn from ensembles of random two-body matrix elements. Many features of pairing that are commonly attributed to the interaction are in fact seen in a large part of the ensemble space. Not only do the spectra show evidence of pairing with favored $J=0$ ground states and an energy gap, but the relationship between ground-state wave functions of neighboring nuclei shows signatures of pairing as well. Matrix elements of pair creation-annihilation operators between ground states tend to be strongly enhanced. Furthermore, the same or similar pair operators connect several ground states along an isotopic chain. This algebraic structure is reminiscent of the generalized seniority model. Thus pairing may be encoded to a certain extent in the Fock space connectivity of the interacting shell model even without specific features of the interaction required.

PACS number(s): 21.60.Cs, 05.30.−d, 24.60.Lz, 24.10.Cn

I. INTRODUCTION

Pairing in fermion systems is a ubiquitous phenomenon that appears among fermions as diverse as electrons, nucleons, and ^{3}He atoms. In the nuclear shell model this is usually explained as being due to strong, attractive matrix elements of the two-body effective interaction between $\mathcal{J}=0$ pair states. In the Fermi-liquid model it is explained as a consequence of the interaction being attractive at certain momentum and energy transfers. In this paper we wish to demonstrate that features of pairing arise from a very large ensemble of two-body interactions and, hence, are independent, to a large extent, from the specific character of the interaction. Pairing may be favored simply as a consequence of the two-body nature of the interaction and the way it connects the Fock space wave functions of the noninteracting fermion system. We examine this possibility by numerical studies of the many-body system governed by a two-body Hamiltonian taken from a random ensemble. We consider nucleons in a spherical shell-model space for which $\mathcal{J}=0$ states have a special significance. We thus take ensembles of two-body Hamiltonians that respect angular momentum, but otherwise are as general as possible.

In an earlier paper [1], we examined spectral features of pairing with one such ensemble and found that two signatures were present in the preponderance of Hamiltonians: the ground state tends to have $J=0$ angular momentum, and there tends to be a gap between that state and the higher states in the spectrum. We use $\mathcal{J}$ to represent the total angular momentum of the two-body matrix-elements, and J to represent the many-body ground states. Another important feature shown in [1] was referred to as phonon collectivity. Ground states with $J=0$ had, on the average, rather large matrix elements of a single-nucleon operator with the first excited $J=2$ states. This is a spectral characteristic of pairing, but it may occur in other situations as well. Why pairing

should be favored in a general ensemble is not clear. It has been suggested that time-reversal invariance is responsible [2], but that symmetry has been found to be unnecessary [3]. In any case, energy spectra are only part of the properties affected by pairing. The term ''pairing'' implies that the ground state can be approximated or modeled by a condensate of pairs of fermions coupled, in the interacting shell model, to zero angular momentum; that is, the ground state is approximately of the form $(\Sigma_{\alpha,m} c_\alpha a^\dagger_{\alpha,m} a^\dagger_{\alpha,-m})^N |0\rangle$. Furthermore, under some conditions the matrix elements of pairing operators have an algebraic structure, as described by the seniority model and its generalizations (see [4]). Along these lines, we consider here two signatures that explicitly probe the wave functions:

A strong pair-transfer amplitude; that is, there is a large matrix element of the pair annihilation operator between the ground states of the nuclei with $A-2$ and A nucleons;

Considering an isotopic chain of nuclides together, A, $A-2$, $A-4$, etc., the seniority model and its generalizations predict that the same pair annihilation operator that takes one from the A ground state to the $A-2$ ground state will also take one from the $A-2$ to the $A-4$ ground state, etc.

We also consider here an additional energy signature: in an isotopic chain containing both even and odd A, the even isotopes have systematically greater binding energies.

Besides considering these three additional signatures of pairing, we will examine some other ensembles to see how robust our results are. The calculations are performed in two shell-model spaces: the ''sd'' space consisting of the orbitals with angular momentum $j=1/2,3/2,5/2$ which can accommodate up to 12 identical particles, and the ''pf'' space which has in addition the $j=7/2$ shell and accommodates up to 20 identical particles. We use the Glasgow–Los Alamos [5] and ANTOINE shell-model codes [6] to calculate the many-body wave functions and observables in these shell-model spaces. The Hamiltonian is specified by the single-particle and two-

particle matrix elements. Except for one ensemble discussed below, we set the single-particle matrix elements to zero.

II. TWO-BODY RANDOM INTERACTIONS

For the two-body matrix elements, we choose a basis of two-body states, labeled by α, which has good angular momentum $\mathcal{J}$. There are 63 independent two-body matrix elements in the sd space and 195 in the pf space, including both neutrons and protons. We define an ensemble of two-particle Hamiltonians requiring that the ensemble be invariant under changes in the basis of two-particle states. This can be achieved by taking the matrix elements to be Gaussian distributed about zero with the widths possibly depending on $\mathcal{J}$,

$$\langle V_{\alpha,\alpha'}^2 \rangle = c_{\mathcal{J}_\alpha}(1 + \delta_{\alpha,\alpha'})\bar{v}^2, \qquad (1)$$

$$\langle V_{\alpha,\alpha'} V_{\beta,\beta'} \rangle = 0, \quad (\alpha,\alpha') \neq (\beta,\beta').$$

Here $\bar{v}$ is an overall energy scale that we generally ignore (except for scaling single-particle energies for the RQE-SPE defined below). The coefficients $c_{\mathcal{J}}$ then define the ensemble. We emphasize that $\mathcal{J}$ refer to quantum numbers of *two-body* states, and not of the final many-body states (typically 4–10 particles).

We now discuss the choices of ensembles, which may be specified by the $c_{\mathcal{J}}$ coefficients and the single-particle Hamiltonian, if present. In our earlier work we employed the RQE ensemble defined below, but it is important to examine other ensembles to see how robust the results are. The ensembles are:

(1) RQE (random quasiparticle interaction). Here $c_{\mathcal{J}} = (2\mathcal{J}+1)^{-1}$. The relation between the $c_{\mathcal{J}}$ came from imposing an additional invariance on the ensemble, that it be the same for the particle-particle interaction as for the particle-hole interaction [1]. The RQE gives a larger variance to $\mathcal{J}=0$ matrix elements than to the others. Note that even though the variance is larger, the matrix elements are both attractive and repulsive, so there is no bias toward pairing by the traditional mechanism of an attractive two-particle interaction.

(2) TBRE (two-body random ensemble). Here $c_{\mathcal{J}} =$ const. Historically, this was the first two-particle random ensemble to be employed in studying statistical properties of many-particle spectra [7–9].

(3) RQE-NP (random quasiparicle ensemble-no pairing). This is the same as the RQE ensemble, except all $\mathcal{J}=0$ two-body matrix elements are set equal to zero. This ensemble will show clearly whether the $\mathcal{J}=0$ channel matrix elements are needed at all to produce the signatures of pairing. (It is known [4], albeit not widely appreciated, that it is possible to have interactions that are diagonal in seniority without any explicit $\mathcal{J}=0$ pairing interaction.)

(4) RQE-SPE (random quasiparticle ensemble with single-particle energies). All the previous ensembles had the single-particle energies set to zero. Realistic interactions do have nonzero single-particle energies, and these can, in principle, affect pairing properties, at the very least by creating

large shell gaps. For calculations in the sd shell we take here single-particle energies from the Wildenthal interaction [10], scaling $\bar{v} = 3.84$ MeV so as to best match the widths of the two-particle matrix elements. For the pf shell we use single-particle energies from the modified KB3 interaction [11] and scaled $\bar{v} = 4.43$ MeV.

III. RESULTS

For the specific calculations, we considered four, six, and eight neutrons in the sd space; we label these as the corresponding shell-model systems, ^{20}O, ^{22}O, and ^{24}O, respectively; we caution the reader that this labeling can be misleading as we have deliberately put in as little physics of those systems as possible. We also considered four, six, eight, and ten neutrons in the pf space: ^{44}Ca, ^{46}Ca, ^{48}Ca, and ^{50}Ca. Finally, we included systems with nontrivial isospin, considering in the sd-shell four protons and four, six, and eight neutrons: ^{24,26,28}Mg, respectively. In these cases $c_{\mathcal{J}} \rightarrow c_{\mathcal{J}T}$. Thus for the RQE, $c_{\mathcal{J}T} = (2\mathcal{J}+1)^{-1}(2T+1)^{-1}$. For each of these systems, and for each of the ensembles described above, we computed at least 1000 samples.

Spectral signatures. Table I presents the fraction of each ensemble that yields a $J=0$ ground state for the above systems. For purposes of comparison, the fraction of the total many-body states that are $J=0$ and $J=2$ states is also given. If the ground-state spins reflected only the size of the J subspace, there would be more $J=2$ than $J=0$, contrary to our findings.

The angular momentum of the first excited state is also interesting. In cases with a $J=0$ ground state, the first excited state has $J=2$ 50–60 % of the time; for $J>0$, the first excited state is generally $J=0$ or $J=2$ with other low J possible as well.

In addition to a predominance of $J=0$ ground states, such states are pushed down relative to the rest of the spectrum. An example of two spectra from the RQE-NP ensemble is shown in Fig. 1 (Ref. [1] shows a similar figure for the RQE). Note that for spectrum 1(a), the $J=0$ ground state is separated from the excited states by an amount large compared to the average level spacing, while for the case of a $J>0$ ground state, 1(b), the separation of the ground state and the average level spacing is similar.

This is shown in more detail in Fig. 2. Here we define s to be the spacing between the ground state and the first excited state, scaled by the local level spacing D, defined as the ensemble-averaged spacing between the first and second excited states. Because these states in general do not have the same quantum numbers such as total J, one would expect the level spacing to be described by a Poisson distribution, where the probability of finding a spacing s is given by $P(s) = \exp(-s/D)$ [12]. For cases where the ground state $J \neq 0$, the Poisson distribution describes the distribution of s extremely well, as one would predict. For those cases where the ground state is $J=0$, however, the distribution is much broader. It is somewhat approximated by a Poisson, but with D three times larger. We show two cases in Fig. 2. The other nuclides and ensembles yield nearly identical figures. Table

TABLE I. Percentage of ground states for selected random ensembles that have $J=0$ for our target nuclides, as compared to the percentage of all states in the model spaces that have these quantum numbers. (Statistical error is approximately $1-3\%$.) Entries with dashes were not computed.

Nucleus	RQE	RQE-NP	TBRE	RQE-SPE	$J=0$ (total space)	$J=2$ (total space)
^{20}O	68%	50%	50%	49%	11.1%	14.8%
^{22}O	72%	68%	71%	77%	9.8%	13.4%
^{24}O	66%	51%	55%	78%	11.1%	14.8%
^{44}Ca	70%	46%	41%	70%	5.0%	9.6%
^{46}Ca	76%	59%	56%	74%	3.5%	8.1%
^{48}Ca	72%	53%	58%	71%	2.9%	7.6%
^{50}Ca	65%	45%	51%	61%	2.7%	7.1%
^{24}Mg	66%	–	44%	54%	4%	16%
^{26}Mg	62%	52%	48%	56%	4%	15%
^{28}Mg	59%	46%	44%	54%	4%	16%

II tabulates the average $\langle s \rangle$ for the various ensembles. For all cases, a $J=0$ ground state is pushed down an *average* factor of 2.3–3.7 relative to the local level spacing, whereas a $J>0$ ground state is, within statistics, not pushed down at all. Similar results hold for the Mg ensembles.

The third spectral feature is the well-known even-odd staggering of ground-state energies. Figures 3 illustrates the real world situation with the experimental neutron removal energies $S_n(A)=-E(A)+E(A-1)$ of calcium isotopes in the range $A=45-50$. The larger removal energy of the even isotopes is associated with their greater binding energy. We look for evidence of this in our ensemble spectra of the pf isotope chains $A=4-10$ as follows. We first examined the even members of the chain, requiring that all ground states have $J=0$. This is satisfied for $\sim 42\%$ of the members of the RQE ensemble; this is a much larger than expected value $(0.70)^4=0.25$ that one would obtain from Table I assuming that the $J=0$ occurrences are uncorrelated. In the generalized seniority model [4], the even-member ground-state en-

ergies have a quadratic dependence on A, [4] Eq. (23.20):

$$E_{gs}(A)=a+bA+cA^2. \qquad (2)$$

We next make a least-squares fit of the selected even-A chains to this formula. This is, of course, a fit of three parameters to four data points and the description is good. Examples of the deviations about this fit are plotted in Fig. 4. We then computed the binding energies for $n=5,7$. The deviations from Eq. (2) for ^{47,48}Ca are plotted in Fig. 4, scaled to the local level spacing: ^{48}Ca exemplifies all the even-n cases, which are all very similar, while ^{45}Ca yields a plot

FIG. 2. Distribution of ground-state gaps, $s=E_1-E_0$, in the spectrum of ^{48}Ca and ^{22}O. Energies are scaled to the average local level density defined as the inverse level spacing between the first and second excited states, $D=\langle E_2-E_1 \rangle$ (averaged over the ensemble). The dashed histogram is the distribution for the cases in which the ground state has nonzero spin, and the dashed curve is the expected Poisson distribution. For ^{22}O we give the distribution for $J=2$ ground states; all other $J>0$ ground states have essentially identical distributions. The solid histogram shows the case for $J=0$ in the ground state. This is also rather well fitted by a Poisson curve (solid), but in this case with an average level spacing three times larger.
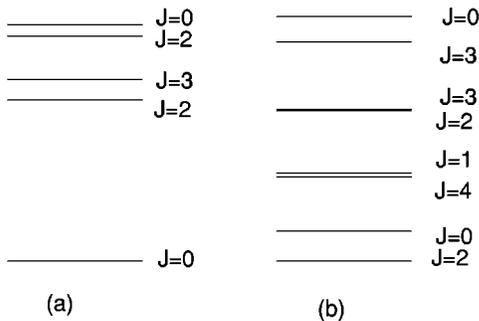

FIG. 1. Typical spectra for ^{22}O with an RQE Hamiltonian: (a) an example with the $J=0$ ground state; (b) an example with the $J\neq 0$ ground state. Note the absence of a ground-state gap in the $J\neq 0$ case. (Energy scale is arbitrary.)
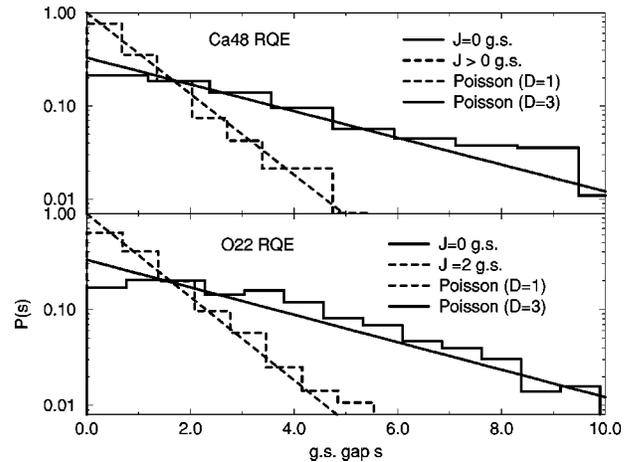
TABLE II. Average gap between $J=0$ ground state and first excited states $\langle s \rangle$ scaled by the local level spacing (computed from the first and second excited states). The same quantity computed for $J>0$ ground states is between 0.9 and 1.2 for all cases considered.

Nucleus	RQE	RQE-NP	TBRE	RQE-SPE
^{20}O	2.7	2.5	2.3	2.3
^{22}O	3.2	2.8	2.8	3.4
^{24}lO	2.9	2.5	2.3	3.7
^{44}Ca	3.1	2.6	2.4	3.1
^{46}Ca	3.8	3.2	3.0	3.6
^{48}Ca	3.4	3.0	3.5	3.5
^{50}Ca	3.5	3.0	3.0	3.4

nearly identical to that of ^{47}Ca. Notice that not only are the odd-particle systems consistently higher in energy, they are pushed up on average by three times the local level spacing — which is entirely consistent with the results shown in Fig. 2 and Table II. Figure 4 also contains results from the RQE-NP ensembles in the pf shell. Even with all $\mathcal{J}=0$ matrix elements set to zero, we find qualitatively similar results. The effects are not as dramatic in this case; from Table I one would expect all four isotopes ^{44,46,48,50}Ca to have $J=0$ ground states 6.5% of the time, but in fact this occurs 8.4 ± 0.8% of the time.

Pair-transfer collectivity. The spectral and energetic characteristics discussed above are not the only signatures of pairing; matrix elements of pairing operators are also very important. In order to test the hypothesis that the ground states of these random Hamiltonians can be approximated by pair condensates, let us follow the example of generalized seniority and consider the general pair-annihilation operator $S = \Sigma_j \alpha_j S_j$, where $S_j = \Sigma_{m>0}(-)^m a_{jm} a_{j-m}$ is the pair-annihilation operator for the j shell. Given S, the pair-transfer amplitude from the ground state with A particles to $A-2$ particles is $\langle A-2|S|A \rangle$. One way to probe the wave function is the *pair-transfer fractional collectivity* (defined in analogy with the phonon fractional collectivity of Ref. [1]):

$$f_p = \frac{\langle A-2|S|A \rangle^2}{\langle A|S^\dagger S|A \rangle}. \tag{3}$$

If the states of the system are condensates of the $S^\dagger$ pairs, then one expects $f_p = 1$.
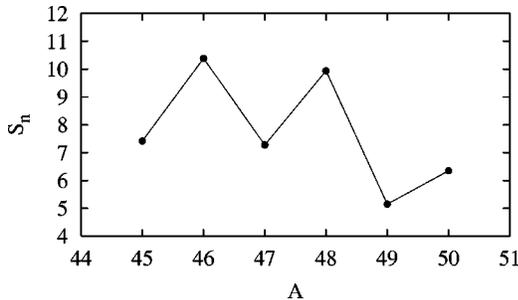
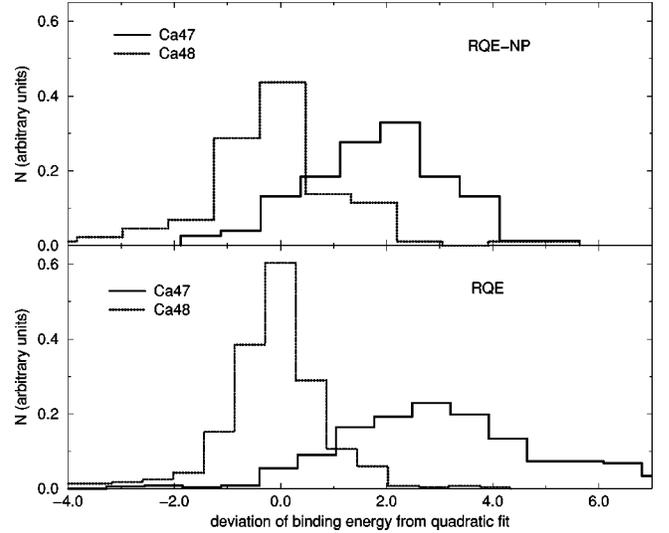FIG. 3. Experimental neutron separation energies of Ca isotopes in the range $A = 45-50$.

FIG. 4. Even-odd staggering effect in the RQE and RQE-NP for 4–10 neutrons in the pf shell.

How does one determine the α_j? Because the ensembles are defined to be invariant on changes of basis, there cannot be a globally preferred α_j. In principle, we could determine individual α_j for each ensemble member by maximizing f_p from Eq. (3). However, the variational condition is rather complicated, and we found satisfactory evidence of pairing collectivity with a much simpler ansatz. In analogy to the phonon fractional collectivity used in [1], we set

$$\alpha_j = \langle A-2|S_j|A \rangle. \tag{4}$$

Figure 5 presents the distribution of the f_p for various nuclides and interaction ensembles. The ensemble denoted GOE refers to using two different RQE interactions for the A and $A-2$ wave functions; one would expect a minimal correlation between their wave functions and indeed the distribution of f_p is heavily weighted towards zero for all nu-
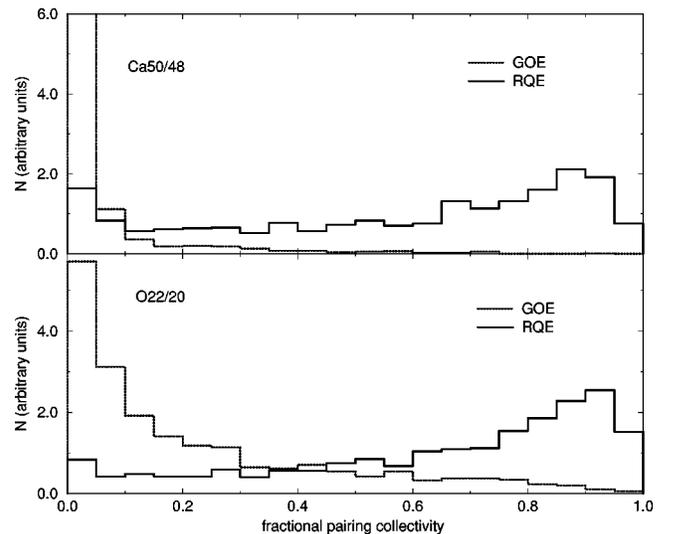
FIG. 5. Distribution of fractional pair-transfer collectivity f_p for selected isotopes and ensembles.

TABLE III. Average value of fractional pair-transfer collectivity f_{pair} between nuclides A and $A-2$. Realistic denotes Wildenthal interaction for sd shell nuclides and KB3 interaction for pf shell nuclides. GOE denotes pair-transfer amplitudes between random wave functions; that is, A and $A-2$ were computed using different members of the RQE ensemble.

Nucleus initial→ final	Realistic	GOE	RQE	RQE-NP	TBRE	RQE-SPE
$^{24}\text{O} \rightarrow {}^{22}\text{O}$	0.99	0.25	0.77	0.75	0.78	0.86
$^{22}\text{O} \rightarrow {}^{20}\text{O}$	0.86	0.22	0.65	0.59	0.62	0.77
$^{50}\text{Ca} \rightarrow {}^{48}\text{Ca}$	0.98	0.032	0.57	0.42	0.47	0.58
$^{48}\text{Ca} \rightarrow {}^{46}\text{Ca}$	0.86	0.036	0.51	0.34	0.38	0.53
$^{46}\text{Ca} \rightarrow {}^{44}\text{Ca}$	0.94	0.070	0.48	0.28	0.30	0.48
$^{28}\text{Mg} \rightarrow {}^{26}\text{Mg}$	0.57		0.26	0.15		0.27
$^{26}\text{Mg} \rightarrow {}^{24}\text{Mg}$	0.72		0.39	0.27		0.47

FIG. 6. Distribution of the correlation angle (see text for definition) between neighboring pair-transfer amplitudes.

clides. For the cases using the same interaction for the A and $A-2$ wave functions, however, we get distinctly different results: a weighting towards $f_p=1$, implying an enhanced correlation indicative of a pairinglike condensate. All our nuclides and ensembles yield similar plots. The results are summarized in Table III in the form of the average fractional pairing. Keep in mind that the distributions for GOE have a negative slope, while for all other ensembles the slope of the distribution is positive. (We also tabulate, for comparison, the exact f_p for realistic interactions: the Wildenthal interaction [10] in the sd shell and modified KB3 [11] in the pf shell.) Thus, in the cases of Ca and O, for all these ensembles—even those with the $\mathcal{J}=0$ pairing matrix elements explicitly removed—we see an increased enhanced number of states with a condensatelike ground state. The Mg nuclei lie in between the GOE and ensembles of identical nucleons. This indicates that the proton-neutron interaction dampens the pairing collectivity present in all-neutron systems such as the $^{20-24}\text{Ca}$ and $^{44-50}\text{Ca}$ isotopes. The difference is likely due to the $T=0$ interaction.

For interactions that are truly diagonal in generalized seniority, one expects the *same* condensate to prevail for $A=2,4,6,8,\ldots$ valence nucleons [4]. In the language developed above, let $\alpha_j(A)$ be the coefficients computed from A and $A-2$. The $\{\alpha_j(A)\}$ can be thought of as vectors, and from generalized seniority we expect the vectors $\vec{\alpha}(A)$ and $\vec{\alpha}(A+2)$ to be aligned. To test this idea, define the scalar product $\vec{\alpha}(A)\cdot\vec{\alpha}(A')=\Sigma_j\alpha_j(A)\alpha_j(A')$, where the states and matrix elements are calculated with the same two-body Hamiltonian. (One could have different weightings or metrics for this scalar product, such as $\sqrt{2j+1}$ or $1/\sqrt{2j+1}$, but such differences in definition do not change our results.) Then plot the distribution of

$$\cos\theta = \frac{|\vec{\alpha}(A)\cdot\vec{\alpha}(A+2)|}{|\alpha(A)||\alpha(A+2)|}. \quad (5)$$

Calculations for the O and Ca isotopes using realistic interactions [8,9] typically give 0.99 for this correlation factor, except at shell closures of the $d_{5/2}$ in the sd shell and $f_{7/2}$ in
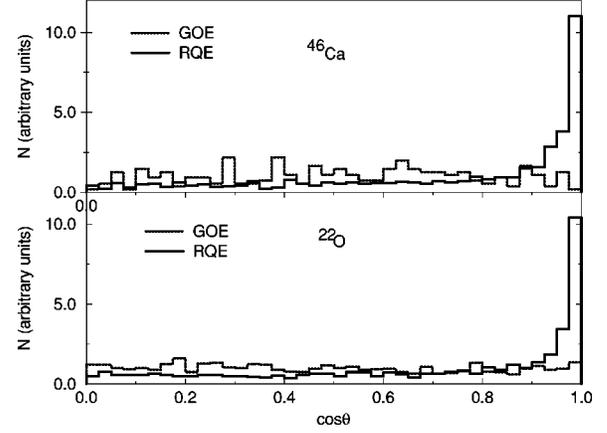
the pf shell, where it is 0.4–0.5. For the Mg isotopes with the Wildenthal interaction, this factor is 0.7, indicating that the likelihood for the same correlated pair to be transferred along the chain is somewhat less than the all-neutron case. If all $T=0$ matrix elements are set to zero, then one recovers the factor 0.99 for the correlation. The results for the GOE and RQE ensembles for O and Ca are plotted in Fig. 6. For the GOE case we find a flat distribution — the pair-transfer amplitudes are uncorrelated, exactly as one would expect. However, for the ensembles of random two-body interactions, we find for the O and Ca chains a sharp peak at 1, indicating a strong correlation. The chain $^{28}\text{Mg}\rightarrow{}^{26}\text{Mg}\rightarrow{}^{24}\text{Mg}$, plotted in Fig. 7(b), also shows a peak at 1, which is a factor of 4 higher than the average bin height. In contrast, the O and Ca peaks are at least a factor of 10 above the average bin height. Thus, the pair transferred in the O and Ca
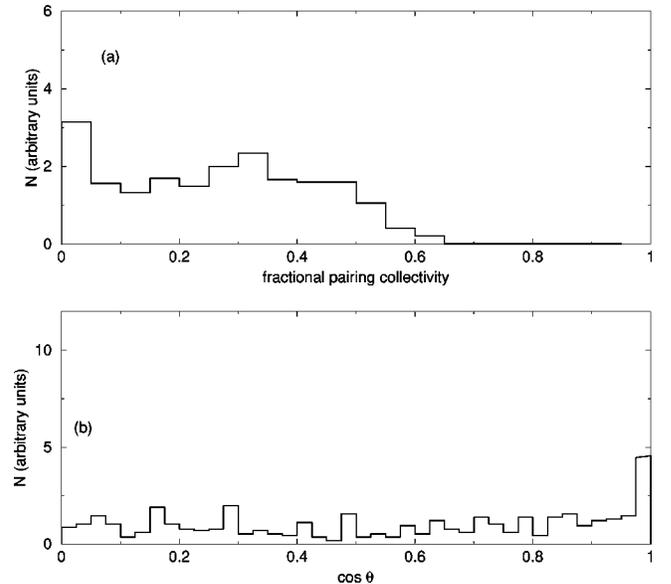

FIG. 7. Results for Mg isotopes. (a) Same as Fig. 5, for RQE. Fractional pair-transfer collectivity for $^{26}\text{Mg}\rightarrow{}^{24}\text{Mg}$. (b) Same as Fig. 6, for RQE. Distribution of correlation angle for $^{28}\text{Mg}\rightarrow{}^{26}\text{Mg}$ and $^{26}\text{Mg}\rightarrow{}^{24}\text{Mg}$.

chains is much more likely to be of the same condensates than the pair transferred in the Mg case. The other ensembles yield plots similar to that shown for the RQE. Curiously enough, for the RQE-NP ensemble (not shown), we also find a sharp peak at $\cos\theta = 0$, as well as at $\cos\theta = 1$.

The analysis described in the previous paragraph only considered ''nearest-neighbor'' transitions. If, however, we have an approximate generalized seniority, then we expect the pair-transfer amplitude vector to be similar for a whole chain of isotopes. We compare, for the RQE, the correlation for the pair-transfer amplitudes starting from $^{50}\text{Ca}\rightarrow{}^{48}\text{Ca}$ and computing the correlation, not only with $^{48}\text{Ca}\rightarrow{}^{46}\text{Ca}$, but also with $^{46}\text{Ca}\rightarrow{}^{44}\text{Ca}$. This correlation shows an enhancement at the value that is similar to the results shown in Fig. 6. Thus we have strong evidence that the pairing condensate is not an arbitrary and local feature, but persists along an isobaric chain.

IV. CONCLUSIONS

We have considered several random ensembles of two-body Hamiltonians in the framework of the shell model. By examining the statistical properties of the low-lying spectra, as well as pair-transfer amplitudes, we find pairing behavior occurs frequently in our ensembles of two-body interactions. Thus, pairing is a robust feature of two-body Hamiltonians. There seems to be a large class of two-body interactions leading to pairing which is much wider than the attractive interactions usually considered.

Besides pairing, there are other features of nuclear spectra that often occur and can give rise to algebraic structures. The most prominent example, rotational bands, is not favored at all by random Hamiltonians. Since a rotational band implies an internal rigidity of the system, this shows that in some sense the random ensembles describe only Fermi-liquid behavior. In the spherical shell model, it has been shown that it is the $T=0$ part of the nuclear effective interaction acting between neutrons and protons which gives rise to collective spectra like the rotational ones. The effective $T=0$ interaction has a rather strong quadrupole component which breaks the seniority coupling scheme.

It is interesting to speculate on the more complex algebraic structures that have been found in nuclear spectroscopy. The phenomenologically successful interacting boson model is based on collective pair transfer operators in both $J=0$ and $J=2$ (quadrupole) angular momenta. It might be that the important physical features could be described very simply, say, by an attractive surface delta interaction. One would then look for the rich variety of observed dynamical symmetries by adding to the physical component a component from one of the random ensembles.

[1] C.W. Johnson, G.F. Bertsch, and D.J. Dean, Phys. Rev. Lett. **80**, 2749 (1998).

[2] W. Haxton (private communication).

[3] R. Bijker, A. Frank, and S. Pittel, Phys. Rev. C **60**, 021302 (1999).

[4] I. Talmi, *Simple Models of Complex Nuclei* (Harwood, New York, 1993).

[5] R.R. Whitehead, A. Watt, B.J. Cole, and L. Morrison, Adv. Nucl. Phys. **9**, 29 (1988).

[6] Code ANTOINE, E. Caurier, Strasbourg, 1989.

[7] O. Bohigas and J. Flores, Phys. Lett. **34B**, 261 (1971).

[8] O. Bohigas and J. Flores, Phys. Lett. **35B**, 383 (1971).

[9] J.B. French and S.S.M. Wong, Phys. Lett. **33B**, 449 (1970).

[10] B.H. Wildenthal, Prog. Part. Nucl. Phys. **11**, 5 (1984).

[11] A. Poves and A.P. Zuker, Phys. Rep. **70**, 235 (1981); E. Caurier, K. Langanke, G. Martinez-Pinedo, and F. Nowacki, Los Alamos preprint nucl-th/9903042.

[12] T.A. Brody *et al.*, Rev. Mod. Phys. **53**, 385 (1981).